

CrystEngComm

Accepted Manuscript



This is an *Accepted Manuscript*, which has been through the Royal Society of Chemistry peer review process and has been accepted for publication.

Accepted Manuscripts are published online shortly after acceptance, before technical editing, formatting and proof reading. Using this free service, authors can make their results available to the community, in citable form, before we publish the edited article. We will replace this *Accepted Manuscript* with the edited and formatted *Advance Article* as soon as it is available.

You can find more information about *Accepted Manuscripts* in the [Information for Authors](#).

Please note that technical editing may introduce minor changes to the text and/or graphics, which may alter content. The journal's standard [Terms & Conditions](#) and the [Ethical guidelines](#) still apply. In no event shall the Royal Society of Chemistry be held responsible for any errors or omissions in this *Accepted Manuscript* or any consequences arising from the use of any information it contains.

ARTICLE

Manipulation on ZnO heterostructures: from binary ZnO-Ag to ternary ZnO-Ag-polypyrrole

Cite this: DOI: 10.1039/x0xx00000x

Juan Li,^a Jian Yan,^a Chengzhan Liu,^a Lihong Dong,^b Hui Lv,^c Wendong Sun,^{*a} and Shuangxi Xing^{*a}

Received 00th January 2012,

Accepted 00th January 2012

DOI: 10.1039/b000000x

www.rsc.org/

A fast reaction between zinc acetate and hexamethylenetetramine was carried out to produce peanut-shaped ZnO-Ag heterostructures in ethylene glycol/water mixed solvent using Ag nanoparticles as seeds and polyvinylpyrrolidone as surfactant. The Ag nanoparticles were well-dispersed on the ZnO particles, endowing them better photocatalytic performance in the decomposition of methylene blue than the pure ZnO. Furthermore, the introduction of a polypyrrole coating layer on the ZnO-Ag surface enhanced the catalytic activity in two ways. On one hand, polypyrrole could protect the Ag from oxidation and being lost under both UV irradiation and visible light. On the other hand, polypyrrole could prominently increase the absorption of photons under the visible light.

Introduction

Constructing effective photocatalysts have attracted more and more attentions in solving the increasingly serious environmental issues, which is caused by the organic effluents from the fabrics and other industries. Zinc oxide has been proved to be a good candidate for its catalytic efficiency, low cost, and environment sustainability. However, the wide band gap (3.37 eV) makes ZnO present limited catalytic performance. In order to improve its catalytic activity, one way is to lower down the size of the ZnO materials to micro/nanometers¹ or construct porous structure.² In the above senses, much more active sites are available to achieve high catalytic effect. On the contrary, aggregation often becomes inevitable due to the high surface area and activity, which decreases the photodegradation effect. The other way is to effectively hinder the recombination of photogenerated electrons and holes. In this case, noble metals,^{3,4} metal oxides,^{5,6} polymers⁷ or carbon materials⁸⁻¹⁰ have been adapted to act as electron trapping agents via combined with ZnO materials. Among them, the noble metal/ZnO heterostructure prevails because the optical vibration of surface plasmon in noble metals results in the oscillation of the free electrons and leads to a strong light scattering and enhancement in the photocatalytic reaction.¹¹ Besides, a Schottky barrier is formed between ZnO and noble metals, which originates from their different work functions and band alignments. This barrier can suppress the recombination of electrons and holes in photocatalytic reaction.

Among all the metals, silver nanoparticle is a popular choice owing to its excellent optical and electrical properties. Up to

now, kinds of ZnO-Ag composites with different morphologies have been prepared through a variety of methods.¹²⁻¹⁴ Generally, the Ag located in the central part of the composite as a core via a seed-growth manner¹⁵ or attached on the surface of the ZnO by a deposition process.^{16,17} In the first case, the contact between the dye molecules and the active components might be hampered in certain degree; in the second one, the metal nanoparticles turned to migrate and aggregate due to their high surface energy. Therefore, it is necessary to construct a novel heterostructure, where the silver nanoparticles are highly separated and the ZnO surface presents high active sites. For this purpose, we designed an appropriate system to achieve unique peanut-shaped ZnO particles decorated by highly-dispersed Ag nanoparticles using zinc acetate and hexamethylenetetramine as reactive sources and polyvinylpyrrolidone as surfactant in ethylene glycol/water mixed solvent. Furthermore, the silver nanoparticles were protected by a thin polypyrrole (PPy) layer to keep them away from aggregation, oxidation or lost. The products exhibited superior property in the photodegradation of MB under UV irradiation or visible light after wrapped by the PPy film.

Experimental

Materials

Solutions used in the experiment were prepared with ultrapure water (resistivity > 18 MΩ·cm⁻¹) or ethylene glycol (EG). Pyrrole (98%, J&K Chemical Ltd) was distilled before use and stored at 4 °C. Zinc acetate dihydrate (99%, Xilong Chemicals), silver nitrate (99.8%) and polyvinylpyrrolidone (PVP k-30,

Sinopharm Chemical Reagent Co.Ltd), hexamethylenetetramine (HMT, 99%, Acros), dodecyl sulfate sodium salt (SDS, 99%, J&K Chemical Ltd) were used as received.

Preparation of Ag seeds

Briefly, 0.025 g of AgNO_3 and 0.1 g of PVP were dissolved in 10 ml of ethylene glycol. The mixture was ultra-sonicated for 10 min to facilitate the dissolving of PVP and AgNO_3 in EG. Then, the reaction system was put into an oil bath at 160° . After maintaining at this temperature for 3 hrs under stirring, the reaction system was cooled down to room temperature.

Synthesis of ZnO-Ag

The reagents mentioned in the portion were all dissolved in EG before used. The typical method to synthesize ZnO-Ag was as followed: 1 mL of $\text{Zn}(\text{Ac})_2 \cdot 2\text{H}_2\text{O}$ (100 mM), 2 mL of HMT (50 mM) and 2.5 mL of PVP (20 mM in monomer concentration) were mixed in EG/ H_2O (v:v=3:4), which contained 0.5 mL of as-synthesized Ag colloid. The mixture in a 25 ml flask was stirred for ten minutes at room temperature. Then it was refluxed at 160° under stirring. After 15 min, the heat source was removed and the reaction vessel was cooled down to room temperature. The products were collected by centrifugation and washed for several times with acetone, ethanol and water successively. Finally, the products were dried at 80° for further characterizations and applications. For the sake of comparison, the pristine ZnO were also synthesized under the same conditions in the absence of Ag seeds.

Coating with PPy thin film

10 mg of ZnO-Ag was dispersed in a mixture containing 20 ml of pyrrole (2.5 mM) and 1 ml of SDS (40 mM) with the help of ultrasonic. After that, 10 ml of AgNO_3 (5 mM) aqueous solution was added to the mixture followed by ultrasonic for 30 min. Then the reaction system was incubated at room temperature for 24 hrs. During the process, the color of the system changed from brown to black slowly, indicating the polymerization of pyrrole. The products were obtained by centrifugation and washed with water and ethanol for several times. Finally, the products were dried in an oven at 50° for 12 hrs.

Characterization

The morphologies of the samples were recorded using a field-emission scanning electron microscope (FESEM, XL-30 ESEM FEG) and a transmission electron microscope (TEM, JEOL 2100F). The X-Ray powder diffraction (XRD) patterns of the products were recorded on a Rigaku D max diffraction system with high-intensity Cu K α radiation. The UV-vis spectra of the products were detected with a UV-vis spectroscopy (UV-2550). Fourier transform infra-red (FT-IR) spectrum was collected at room temperature with a Bruker IFS 66 V instrument.

Photocatalytic evaluation

Methylene blue (MB) was selected as a model dye to evaluate the photocatalytic activity of the samples. In UV light catalysis experiment, 12 mg of products were dispersed in 40 ml of MB aqueous solution (10 ppm). Prior to photoreaction, the suspensions were magnetically stirred in dark for about 30 min to attain the adsorption-desorption equilibrium. Then the system was irradiated by a 300w high-pressure mercury lamp with an average power density of 3.39 mW cm^{-2} on the samples. 2 ml of sample aliquots was extracted from the mixture solution at a certain time interval, and subsequently centrifuged at 8000 rpm for 6 min to separate the catalysts. The degradative capability of the catalysts was measured by UV-vis spectrum. In the case of the visible light, the photocatalytic experiment was conducted under the same conditions except that the dosage of the catalyst was changed from 12 mg to 5 mg. Meanwhile, to evaluate the photocatalytic lifetime of the products, the photoreaction was performed under UV irradiation and visible light up to four cycles.

Result and Discussion

Structure and Morphology

The XRD patterns of the pure ZnO, ZnO-Ag and ZnO-Ag-PPy are shown in Figure 1. The well defined diffraction peaks display the crystalline nature of the samples. The peaks marked with \circ in curve 1 demonstrate that the pristine ZnO possesses a hexagonal wurtzite structure (JCPDS card no. 36-1451). No other peaks are detected, indicating the high purity of the product. When the synthesis proceeds in the presence of Ag seeds, additional peaks appear at 38.2° , 44.4° , 64.6° (curve 2 and 3 with the mark of \blacklozenge), which correspond to (111), (200) and (220) crystal planes of face-centered cubic (fcc) structured Ag, respectively (JCPDS card no. 04-0783).

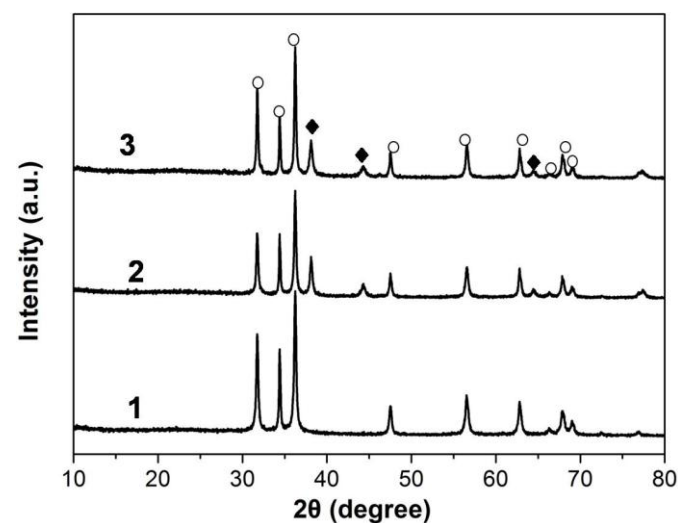


Figure 1. XRD patterns of (1) ZnO; (2) ZnO-Ag; (3) ZnO-Ag-PPy.

The existence of PPy was investigated by FT-IR spectrum (Figure 2a). The peaks at about 1504 and 1389 cm^{-1} correspond

to the C-C and C-N stretching vibrations in the pyrrole ring, respectively. The peak displaying at about 1226 cm^{-1} represents

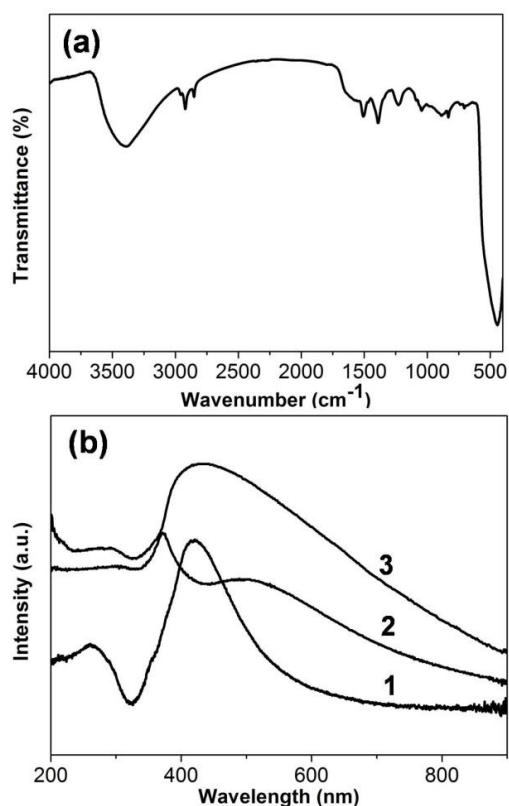


Figure 2. (a) FT-IR spectrum of the ZnO-Ag-PPy, (b) UV-vis spectra of Ag (1), ZnO-Ag (2) and ZnO-Ag-PPy (3).

the plane vibration of $=\text{CH}-$. Meanwhile, the peaks at 1046 and 891 cm^{-1} attribute to the C-H in-plane and of the above peaks confirms the successful polymerization of pyrrole.

The UV-vis spectra of the Ag colloid, ZnO-Ag and ZnO-Ag-PPy are shown in Figure 2b. A strong plasmon absorption peak at 422 nm is observed for the Ag colloid and this peak shifts to 500 nm after formation of ZnO-Ag heterostructure. Upon polymerization of pyrrole, a wide band centered at 450 nm is observed, which may originate from the merging of the Ag, ZnO out-of plane deformation vibrations and the bipolaron absorption peak of PPy.¹⁸

The ZnO-Ag composite presents a peanut shape with the length of *ca.* 932 nm and width of *ca.* 455 nm (Figure 3b and e). The Ag nanoparticles ($d_{\text{av}} = 50\text{ nm}$) are separately located on the surface. During the synthesis process, PVP also contributes to the generation of uniform structured ZnO-Ag composites. In the absence of PVP, less peanut shaped ZnO-Ag could be obtained and the products were composed of irregular structure (Figure S1). It confirms that the addition of the PVP is important for the formation of peanut-like structure of ZnO. Many studies have shown that the addition of PVP in the reaction system will affect the kinetics of the growing process, which is due to the formation of the covalent bond between the $-\text{C}=\text{O}$ of PVP and Zn^{2+} .^{19, 20}

In the system, HMT provides an alkaline environment with the help of water, which promotes the formation of ZnO. The hydrolytic processes are as follows:

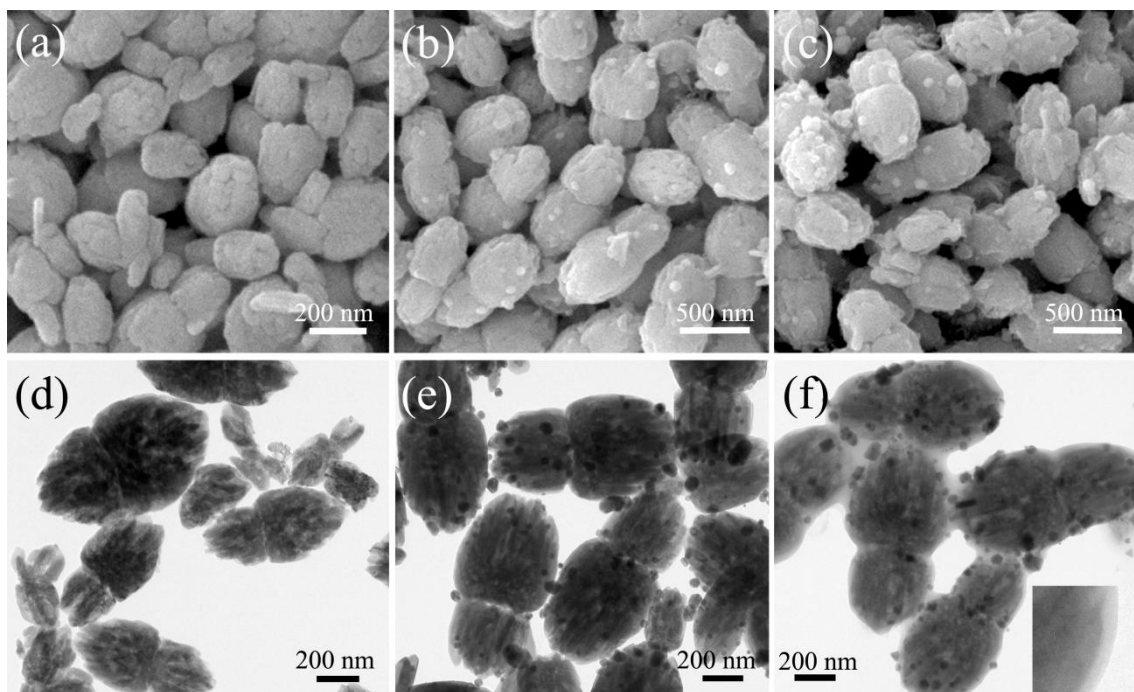
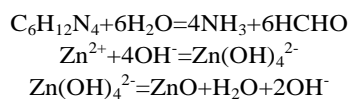


Figure 3. SEM and TEM images of the products. (a, d) ZnO, (b, e) ZnO-Ag and (c, f) ZnO-Ag-PPy. The inset in f is the magnified view shown in the selected area.



After polymerization of pyrrole, a thin layer of PPy is observed with the thickness about 20 nm (inset view of Figure 3f) and the original morphology of the ZnO-Ag maintains as it is. Here, AgNO₃ was selected as the oxidant because it shows weaker oxidizing ability than the commonly used ammonium persulphate, which might oxidize and destroy the Ag nanostructures. On the other hand, the reaction between AgNO₃ and pyrrole produces Ag and PPy simultaneously and the newly formed Ag could be directly deposited on the original Ag surface,²¹ No free PPy or Ag/PPy particles are detected in the whole image, indicating the preferential deposition of Ag and PPy on the ZnO-Ag surface.

Formation mechanism of ZnO-Ag

To make clear how this unique ZnO-Ag structure is formed, a temporal experiment was carried out. In the first 2 min, the newly-formed ZnO assemblies irregularly attached onto Ag nanoparticles (Figure 4a). Along with the further growth process of ZnO components, they have the tendency to attach with each other to lower down the surface-volume energy. As the reaction going on (4 min), lots of hemisphere-shaped ZnO particles are formed owing to the above mentioned possibility and Ostwald ripening process. Meanwhile, the Ag nanoparticles are “doped” onto the ZnO surface without apparent aggregation (Figure 4b). When the reaction time is extended to 6 min, two neighboring hemispheres assemble into peanut-shaped structure in order to further minimize the total surface-volume energy (Figure 4c). The reaction is allowed to continue for 15 min to ensure the complete crystal process (Figure 4d).

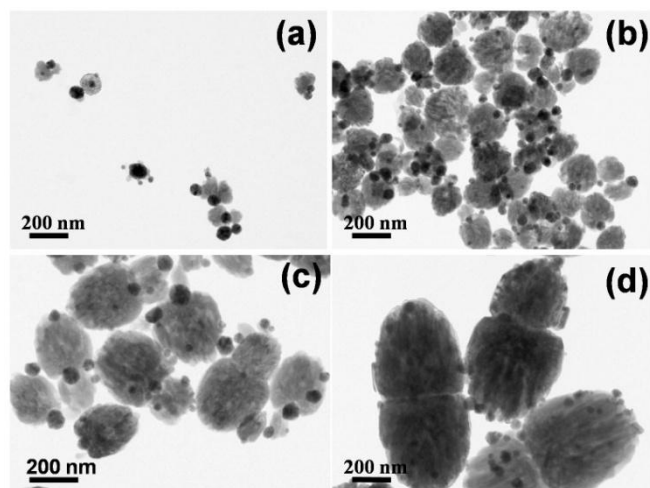


Figure 4. TEM images of the formation process of ZnO-Ag in different reaction time. (a) 2 min, (b) 4 min, (c) 6 min, (d) 15 min.

It should be noted the Ag nanoparticles play important roles in controlling and uniformity of the ZnO particles. In the absence of Ag nanoparticles, the ZnO structure presents a broad

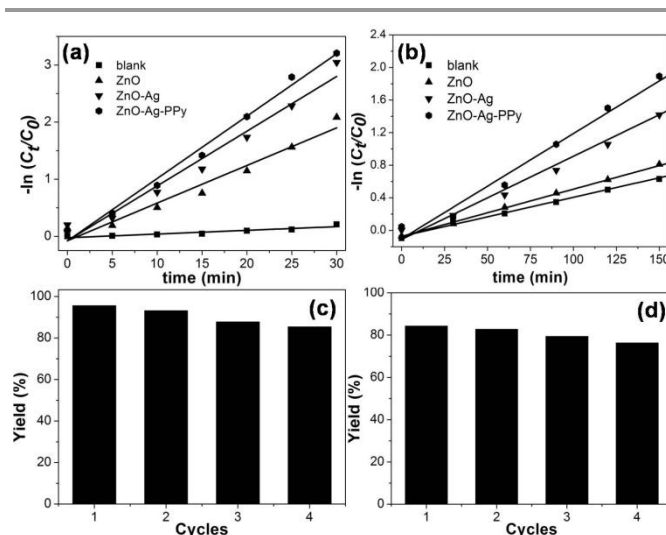


Figure 5. The $-\ln(C_t/C_0)$ versus time curves of photodegradation of MB under UV light (a), and visible light (b) of different products. And the cycling runs for the degradation of MB of ZnO-Ag-PPy under the UV irradiation (c), and visible light (d).

size distribution due to a homogeneous nucleation process that leads to a different growth experience (Figure 3a and d).²² On the contrary, the Ag nanoparticles act as nuclei centers owing to their high activity and lead to the fast assembly of the as-generated ZnO blocks. Finally, a uniform size distribution was obtained.

On one hand, no ZnO could be generated in the absence of HMT, as can be found from the XRD result (Figure S2), where only Ag peaks are observable; on the other hand, the peanut-like structure was hardly produced without water (Figure S3), which means the water can react as the structure-directing agent to induce the formation of unique morphology

Photocatalytic test

Figure 5a shows the photocatalytic properties of ZnO, ZnO-Ag and ZnO-Ag-PPy for the degradation of MB under UV light. In the absence of catalyst, nearly no degradation was detected. Upon addition of ZnO-Ag particles, the intensity of the original peak of the MB at 664 nm decreased and reached 85.3% at 30 min compared with 77.8% for the pure ZnO particles, which is owing to the effective separation of electrons and holes induced by the formation of the ZnO and Ag interface. After depositing a layer of PPy, the catalytic property could be further improved with degradation of 95.6% in 30 min. This should be originated from the PPy protection that hindered the aggregation and lost of the Ag during the catalytic process. To confirm the enhanced performance was not resulted from the newly formed Ag that originated from the reaction between AgNO₃ and pyrrole, a control experiment was carried out using ZnO instead of ZnO-Ag. To avoid misunderstanding, the corresponding product was named as ZnO-PPy. The results showed ZnO-PPy has even worse catalytic performance towards degradation of MB than pure ZnO. (Figure S4a). We consider this comes from two

reasons: 1) The produced Ag did not have strong interaction with ZnO and no apparent synergistic effect could be attained; 2) The PPy layer prevented the contact of MB with the active sites rather than protected the Ag nanoparticles in this case.

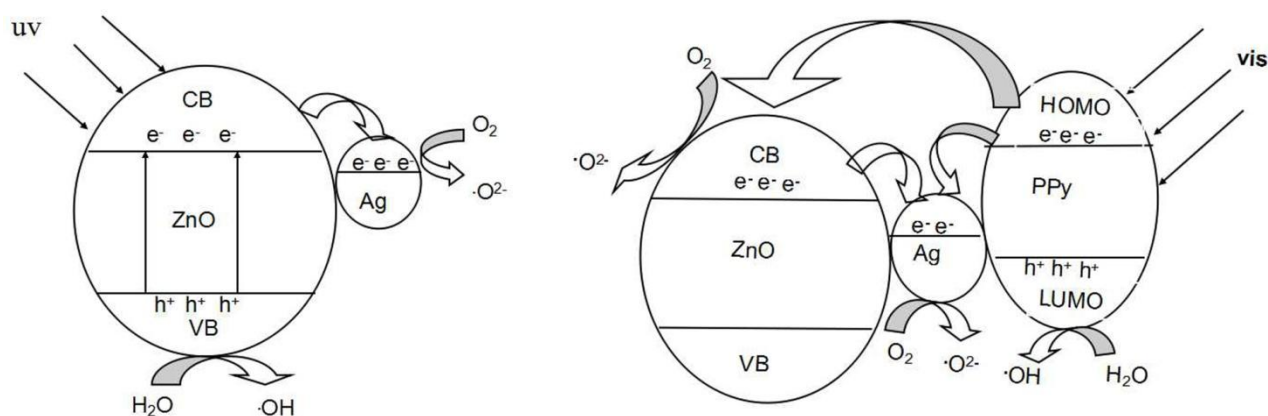


Figure 6. Proposed mechanisms for the degradation of MB of ZnO-Ag-PPy under UV light and visible light.

Considering this reaction a pseudo-first-order reaction, the rate constant (k) is determined by the slope of the linear fit of $-\ln(C_t/C_0)$ vs. t , where C_t/C_0 represents the ratio of MB concentrations upon exposure to UV light irradiation at time t and 0 as calculated based on their corresponding absorption intensity in the kinetic UV-Vis spectra. The obtained k values for pure ZnO, ZnO-Ag and ZnO-Ag-PPy are 0.0658, 0.095 and 0.109 min^{-1} , respectively.

The photocatalytic activity of the different products under visible light was also tested. Among them, the ternary catalyst also exhibits the best catalytic property (Figure 5b). And the k values for ZnO, ZnO-Ag and ZnO-Ag-PPy were calculated as 0.00579, 0.0102 and 0.0129 min^{-1} , respectively. However, the catalytic mechanism might be different under UV and visible light as discussed below.

ZnO is an n-type semiconductor with a wide band gap and it exhibits a strong absorption threshold in the UV region. Under UV light irradiation, electrons are excited from valence band (VB) of ZnO to the conduction band (CB) with holes remaining on the VB. The excited electrons are injected into Ag quickly because the Fermi energy level of Ag is lower than the CB edge of ZnO (Figure 6a). After that, a Schottky barrier is formed at the interface between ZnO and Ag. This makes the charge separation more effective. In the degradation process, electrons transferred from ZnO can be trapped by the absorbed O_2 molecules in water to give $\cdot\text{O}_2^-$ radical. Meanwhile, holes remaining on the VB of ZnO can be scavenged by the H_2O molecules to yield $\cdot\text{OH}$ radicals. These radicals are powerful oxidizing agents for the degradation of MB. The dye molecules that have been absorbed on the catalyst react with these radicals to generate H_2O and CO_2 . In the presence of PPy, we consider it can localize the Ag nanoparticles on their positions to avoid their moving and aggregation during the degradation process.

In the case of visible light, PPy harvests the photons and then excite the electrons from ground state into an excited state with holes leaving in the highest occupied molecular orbital (HOMO) of PPy (Figure 6).²³ Because the level of the lowest unoccupied

molecular orbital (LUMO) is higher than the CB edge of ZnO and the Fermi level of Ag, the excited electrons may be directly injected into these two positions. And electrons of ZnO from PPy prefer to flow into Ag because of the different work functions. Meanwhile, the holes stay in the layer of PPy. As a result, ZnO-Ag-PPy effectively prevents the recombination of photogenerated electrons and holes, and exhibits an excellent photocatalytic activity thereby. As a whole, the enhancement of catalytic ability by depositing a conducting polymer layer onto the ZnO-Ag heterostructure is more effective in causing degradation under visible light than UV irradiation.

These two different mechanisms may be adapted to explain why the ZnO-PPy sample displays different catalytic performances under UV and visible light (Figure S4). In the UV light radiation, PPy are hardly excited and its deposition may contribute negative effect on the catalytic performance depending on the interaction between the Ag and ZnO. However, PPy participates in the whole catalytic process in the case of visible light radiation and a better result than that of ZnO-Ag can be achieved (Figure 5b).

In order to test the lifetime of the catalysts, the recycled behavior of the ZnO-Ag-PPy was studied for up to four runs under both UV light and visible light. As shown in Figure 5c and d, the catalytic property of ZnO-Ag-PPy still remained 85.4% and 76.3% after four cycles under the irradiation of UV and visible light, respectively. Apart from that, the stability of ZnO-Ag was carried out under UV irradiation to make clear the difference between the binary and ternary heterostructure and the results showed the ZnO-Ag-PPy still presented higher catalytic performance than that of ZnO-Ag (81 %, Figure S5) after four cycles, indicating the protection of PPy layer on the surface of ZnO-Ag. It should be noted that part of the generated CO_2 can react with ZnO, which produces ZnCO_3 during the catalysis process, and we consider it may be a possible reason to result in the decrease of photocatalytic properties.

Conclusions

In summary, a novel ternary photocatalyst ZnO-Ag-PPy was successfully synthesized by a fast reaction followed by a chemical polymerization method. The reaction between zinc acetate and hexamethylenetetramine in ethylene glycol /water mixed solvent in the presence of polyvinylpyrrolidone and AgNO₃ induced the generation of peanut-like ZnO-Ag heterostructure. The following reaction between silver nitrate and pyrrole on the surface of ZnO-Ag led to the final ZnO-Ag-PPy products. The introduction of polypyrrole (PPy) to the binary ZnO-Ag was beneficial to achieve enhanced photocatalytic performance both under UV light and visible light. The PPy layer could protect the Ag nanoparticles from moving, aggregation or lost. Meanwhile, when irradiated by visible light, it could help harvest photons and facilitate the separation of photogenerated electrons and holes based on the different work functions among these three components. The ZnO-Ag-PPy proved to be an effective, stable and reusable catalyst, which could be found applications in treatment of environment problems.

Acknowledgements

The authors thank National Natural Science Foundation of China (Grant No. 21103018, 21103126), Jilin Provincial Science and Technology Development Foundation (Grant No. 20140101109JC) and Opening Fund of State Key Laboratory of Rare Earth Resource Utilization from Changchun Institute of Applied Chemistry (RERU2013009) for financial support.

Notes and references

^a Faculty of Chemistry, Northeast Normal University, 5268 Renmin Street, Changchun, P.R. China 130024 Tel: (+86) 85099657; E-mail: xingsx737@nenu.edu.cn; sunwd843@nenu.edu.cn

^b Department of Chemistry, Tonghua Normal University, 950 Yucai Road, Tonghua, P.R. China 134002

^c Jilin Huaqiao University of Foreign Languages, 3658 Jingyue Street, Changchun, P.R. China 130117

† Electronic Supplementary Information (ESI) available: [XRD patterns, photodegradation data, TEM images for control experiments and other data]. See DOI: 10.1039/b000000x/

1. S. Ghosh, D. Majumder, A. Sen and S. Roy, *Mater Lett*, 2014, 130, 215-217.
2. X. Ma, X. Zhang, L. Yang, K. Wang, K. Jiang, Z. Wei and Y. Guo, *CrystEngComm*, 2014, DOI: 10.1039/C1034CE00735B.
3. W. He, H. K. Kim, W. G. Wamer, D. Melka, J. H. Callahan and J. J. Yin, *J Am Chem Soc*, 2014, 136, 750-757.
4. C. Yu, K. Yang, Y. Xie, Q. Fan, J. C. Yu, Q. Shu and C. Wang, *Nanoscale*, 2013, 5, 2142-2151.
5. Q. Xie, Y. Zhao, H. Guo, A. Lu, X. Zhang, L. Wang, M. S. Chen and D. L. Peng, *Acs Appl Mater Interfaces*, 2014, 6, 421-428.
6. S. Balachandran and M. Swaminathan, *J. Phys. Chem. C.*, 2012, 116, 26306-26312.
7. S. S. Barkade, D. V. Pinjari, A. K. Singh, P. R. Gogate, J. B. Naik, S. H. Sonawane, M. Ashokkumar and A. B. Pandit, *Ind Eng Chem Res*, 2013, 52, 7704-7712.

8. C. Han, M. Q. Yang, B. Weng and Y. J. Xu, *Phys Chem Chem Phys*, 2014, DOI: 10.1039/C1034CP02189D.
9. R. Ding, J. Liu, J. Jiang, Y. Li, Y. Hu, X. Ji, Q. Chi, F. Wu and X. Huang, *Chem Commun*, 2009, 4548-4550.
10. R. Zhang, L. Fan, Y. Fang and S. Yang, *J Mater Chem*, 2008, 18, 4964-4970.
11. S. A. Ansari, M. M. Khan, M. O. Ansari, J. Lee and M. H. Cho, *J Phys Chem C*, 2013, 117, 27023-27030.
12. J. Yin, Y. Zang, C. Yue, Z. Wu, S. Wu, J. Li and Z. Wu, *J Mater Chem*, 2012, 22, 7902-7909.
13. S. S. Warule, N. S. Chaudhari, R. T. Khare, J. D. Ambekar, B. B. Kale and M. A. More, *CrystEngComm*, 2013, 15, 7475-7483.
14. W. L. Ong, S. Natarajan, B. Klooster and G. W. Ho, *Nanoscale*, 2013, 5, 5568-5575.
15. C. Gu, C. Cheng, H. Huang, T. Wong, N. Wang and T. Y. Zhang, *Cryst. Growth Des.*, 2009, 9, 3278-3285.
16. Y. Cheng, L. An, J. Lan, F. Gao, R. Tan, X. M. Li and G. H. Wang, *Mater Res Bull*, 2013, 48, 4287-4293.
17. P. Fageria, S. Gangopadhyay and S. Pande, *RSC Advances*, 2014, 4, 24962-24972.
18. S. Xing and G. Zhao, *J Appl Polym Sci*, 2007, 104, 1987-1996.
19. G. Shan, H. Hao, X. Wang, Z. Shang, Y. Chen and Y. Liu, *Colloid Surf. A-Physicochem. Eng. Asp.*, 2012, 405, 1-5.
20. T. Thirugnanam, *J. Nanomater.*, 2013, 2013, 1-7.
21. S. Xing, L. H. Tan, T. Chen, Y. Yang and H. Chen, *Chem. Commun.*, 2009, 1653-1654.
22. S. Xing, Y. Feng, Y. Y. Tay, T. Chen, J. Xu, M. Pan, J. He, H. H. Hng, Q. Yan and H. Chen, *J Am Chem Soc*, 2010, 132, 9537-9539.
23. Y. Yang, J. Wen, J. Wei, R. Xiong, J. Shi and C. Pan, *Acs Appl Mater Interfaces*, 2013, 5, 6201-6207.

Graphic Abstract

A ternary composite ZnO-Ag-polypyrrole was synthesized through a fast reaction between zinc acetate and hexamethylenetetramine followed by an *in situ* surface polymerization process and the sample exhibited a superior catalytic performance in the degradation of methylene blue under both UV irradiation and visible light.

